Identification of Two Tetranuclear FeS Clusters on the Ferredoxin-Type Subunit of NADH:Ubiquinone Oxidoreductase (Complex I)†

Tim Rasmussen,‡,§,|| Dierk Scheide,‡,§ Benedikt Brors,§ Lars Kintscher,§ Hanns Weiss,§ and Thorsten Friedrich*,§

Institut für Biochemie, Heinrich-Heine-Universität, Universitätsstrasse 1, 40225 Düsseldorf, Germany

Received November 27, 2000

ABSTRACT: The proton-translocating NADH:ubiquinone oxidoreductase of respiratory chains (complex I) contains one flavin mononucleotide and five EPR-detectable iron−sulfur clusters as redox groups. Because of the number of conserved motifs typical for binding iron−sulfur clusters and the high content of iron and acid-labile sulfide of complex I preparations, it is predicted that complex I contains additional clusters which have not yet been detected by EPR spectroscopy. To search for such clusters, we used a combination of UV/vis and EPR spectroscopy to study complex I from *Neurospora crassa* and *Escherichia coli* adjusted to distinct redox states. We detected a UV/vis redox difference spectrum characterized by negative absorbances at 325 and 425 nm that could not be assigned to the known redox groups. Redox titration was used to determine the pH-independent midpoint potential to be −270 mV, being associated with the transfer of two electrons. Comparison with UV/vis difference spectra obtained from complex I fragments and related enzymes showed that this group is localized on subunit Nuo21.3c of the *N. crassa* or NuoI of the *E. coli* complex I, respectively. This subunit (the bovine TYKY) belongs to a family of 8Fe-ferredoxins which contain two tetranuclear iron−sulfur clusters as redox groups. We detected EPR signals in a fragment of complex I which we attribute to the novel FeS clusters of complex I.

The proton-translocating NADH:ubiquinone oxidoreductase (complex I;[1] EC 1.6.5.3) is the first energy-transducing complex in the respiratory chains of many procaryotes and most eucaryotes. It couples the transfer of electrons from NADH to ubiquinone with the translocation of protons across the membrane (*1*−*3*). One flavin mononucleotide (FMN) and five EPR-detectable iron−sulfur (FeS) clusters have so far been detected in the complex. The high content of iron and acid labile sulfide (*5*−*7*) as well as the number of conserved sequence motifs that are typical for the binding of FeS clusters would allow the presence of up to three additional FeS clusters that have not yet been detected by EPR spectroscopy. The bacterial complex I, in general, consists of 14 different subunits (*4*). Seven subunits are globular proteins including the subunits that bear the known redox groups of complex I. The remaining seven subunits are highly hydrophobic proteins predicted to fold into 54 α-helices across the membrane. The mitochondrial complex I of eucaryotes contains up to 28 extra proteins in addition to the homologues of the 14 procaryotic complex I subunits (*4*).

Complex I consists of a peripheral arm extending into the water phase and a membrane arm embedded in the lipid bilayer (*8*−*10*). The peripheral arm is involved in the oxidation of NADH by means of FMN, the binuclear FeS cluster N1b, and the tetranuclear FeS clusters N3 and N4 (*7*, *11*, *12*; nomenclature according to Ohnishi). Some organisms contain an additional binuclear cluster N1c to fulfill this function (*7*). The function of the low-potential cluster N1a ($E_{m,7} < -380$ mV) is not known, but it may also be involved in the NADH dehydrogenase reaction. N1b, N1c, N3, and N4 are called isopotential clusters because they show similar midpoint potentials in the range from −240 to −270 mV (*12*). Together with the FMN ($E_{m,7} = -345$ mV; *13*), they form the electron input part of complex I (*4*). Electrons are transferred from the isopotential FeS clusters to the tetranuclear cluster N2, which is located in the connection between the peripheral and the membrane arm. N2 exhibits a more positive midpoint potential than the isopotential clusters, although the respective value depends strongly on the organism complex I has been isolated from (*12*, *14*).

Recently, we detected the presence of two novel redox groups in complex I from *Neurospora crassa* and *Escherichia coli* (*15*−*17*) by means of combined UV/vis and EPR spectroscopy. One is a high-potential group located in the membrane arm of the complex (*15*−*17*). Here, we report that the other novel redox group has a pH-independent midpoint potential of −270 mV and transfers two electrons. Its typical UV/vis difference spectrum is present in fragments of complex I and in related enzymes that contain homologues of subunit Nuo21.3c of the *N. crassa* or NuoI of the *E. coli* complex I, respectively. The bovine homologue is called

† This work is supported by the Deutsche Forschungsgemeinschaft and by the Fonds der Chemischen Industrie.

* To whom correspondence should be addressed. E-mail: thorsten.friedrich@uni-duesseldorf.de. Tel: +49-211-8112647. Fax: +49-211-8115310.

‡ T.R. and D.S. contributed equally to this work.

§ Heinrich-Heine-Universität.

|| Present address: Schools of Chemical and Biological Science, University of East Anglia, Norwich NR4 7TJ, U.K.

[1] Abbreviations: complex I, proton-translocating NADH:ubiquinone oxidoreductase; dodecyl maltoside, *n*-dodecyl β-maltopyranoside; EPR, electron paramagnetic resonance; FeS cluster, iron−sulfur cluster; FMN, flavin mononucleotide.

10.1021/bi0026977 CCC: $20.00
Published on Web 04/28/2001

TYKY (*2*). They belong to a protein family of 8Fe-ferredoxins that contain two tetranuclear FeS clusters as redox groups. Using a fragment of complex I that contains a homologue of TYKY, novel EPR signals were obtained which we attribute to these FeS clusters. From these data we conclude that the novel redox group is made up of the two tetranuclear FeS clusters on TYKY.

MATERIALS AND METHODS

Enzymes. Complex I from *N. crassa* wild-type OR74A was isolated as described (*15*). The peripheral arm of the *N. crassa* complex was isolated from the mutant *nuo*20.9 (*18*) according to ref *19*. The *E. coli* complex I as well as the NADH dehydrogenase fragment and the connecting fragment of this complex were isolated as described (*7*, *20*, *21*). The NAD^+-reducing [NiFe] hydrogenase from *Ralstonia eutropha* (formerly *Alcaligenes eutrophus*; *22*, *23*) and the Ech [NiFe] hydrogenase from *Methanosarcina barkeri* (*24*, *25*) were kind gifts from Drs. B. Friedrich, Berlin, and R. Hedderich, Marburg, respectively. The UV/vis spectra of oxidized and reduced 8Fe-ferredoxin from *Clostridium pasteurianum* (*26*, *27*) were kindly provided by Drs. J. M. Moulis and J. Meyer, Grenoble.

UV/vis Spectroscopy. A TIDAS-UVI/1001-1 diode array spectrometer with 512 diodes (J&M, Aalen, Germany) was used. Measurements were performed with an integration time of 40 ms, and 25 spectra in the range from 200 to 600 nm were accumulated every 0.5 s. Spectra were processed using the Spectrachrom software package (J&M, Aalen, Germany).

UV/vis Spectra of Fully Reduced and Air-Oxidized Complex I. The spectra of complex I in the fully reduced state were obtained under anaerobic conditions in a COY controlled environment chamber (Grass Lake, MI) in 95% N_2 and 5% H_2 as described (*15*). All buffers were degassed 10 times and refilled with argon. Residual traces of oxygen were removed by addition of 10 mM glucose, 23 units/mL glucose oxidase (EC 1.1.3.4, from *Aspergillus niger*, Sigma), and 900 units/mL catalase (EC 1.11.1.6, from bovine liver, Boehringer Mannheim). Two hundred microliter aliquots of 1.7 μM *N. crassa* complex I in 50 mM Tris-HCl and 0.1% dodecyl maltoside (Calbiochem) and 2 μM *E. coli* complex I in 50 mM MES/NaOH, pH 6.0, 50 mM NaCl, and 0.1% dodecyl maltoside were reduced with 170 and 200 μM NADH, respectively. The mixtures were separated on a 1 $\times$ 6 cm Superose 6 column equilibrated in the corresponding buffer containing 1 μM NADH. Spectra of the eluting proteins were continuously measured using the buffer as reference. The spectra of the air-oxidized complexes were obtained in the same way with no NADH added to the enzyme or the buffer (*15*).

Reaction of NADH-Reduced Enzymes with Oxygen. Three milliliter aliquots of 7 μM *N. crassa* complex I in 50 mM Tris-HCl, pH 7.2, and 0.1% dodecyl maltoside were mixed in a stirred optical cell with 30 μM NADH at room temperature. While spectra were continuously recorded, complex I was reoxidized by oxygen from the air. EPR samples were withdrawn every 10 s and immediately frozen. The sampling time was corrected for the handling in order to correlate the UV/vis with the EPR data. UV/vis spectra were obtained in the same way from the 2 μM peripheral arm of *N. crassa* complex I in 50 mM Tris-HCl, pH 7.2, and 0.1% Lubrol WX (ICN), from 2 μM *E. coli* complex I in 50 mM MES/NaOH, pH 6.0, 50 mM NaCl, and 0.1% dodecyl maltoside, from the 10 μM NADH dehydrogenase fragment of the *E. coli* complex I in 50 mM MES/NaOH, pH 6.0, and 50 mM NaCl, and from 10 μM *R. eutropha* NAD^+-reducing hydrogenase in 50 mM Tris-HCl, pH 7.0, and 50 mM NaCl.

Reaction of Dithionite-Reduced Enzymes with Oxygen. Six hundred microliter aliquots of the 2 μM connecting fragment of the *E. coli* complex I in 50 mM MES/NaOH, pH 6.0, 50 mM NaCl, and 0.1% dodecyl maltoside were mixed in a stirred optical cell with a few grains of dithionite at room temperature. While spectra were continuously recorded, the reaction mixture was reoxidized by oxygen from the air. Oxidation of dithionite was followed at 315 nm (*28*). The same experiment was performed with 3 μM Ech hydrogenase from *M. barkeri* in 50 mM MOPS, pH 7.0, 2 mM dithiothreitol, and 1% dodecyl maltoside.

Redox Titration. Redox titrations were performed under strictly anaerobic conditions in a COY controlled environment chamber (Grass Lake, MI) as described above. A 600 μL aliquot of 1.5 μM complex I in 100 mM Tris-HCl and 0.1% dodecyl maltoside was titrated in the range from -300 to -200 mV by addition of 1$-$170 mM lithium lactate and 1$-$10 mM sodium pyruvate. The applied potential was calculated according to the Nernst equation. The midpoint potential for the lactate/pyruvate couple was taken to be -190 mV at pH 7.0 (*29*). As mediator of redox potential, we used 10 units/mL lactate dehydrogenase (LDH, Sigma, type II from rabbit muscle). UV/vis spectra were continuously recorded in a stirred optical cell, and the reaction was started by injection of 5 μM NADH final concentration (grade I, Boehringer Mannheim). This experiment was performed in the range from pH 7.0 to pH 8.2. Midpoint potentials were calculated by fitting a multiple Nernst equation to experimental data (*30*). The calculations were performed with GNUPLOT (*31*). For pH 7.8 the midpoint potential was calculated by means of global analysis of potential-resolved spectral data in the range of 280 to 600 nm (*30*, *32*). Global analysis was performed with the program SPECFIT (Spectrum Software, Chapel Hill, NC; *33*).

EPR Spectroscopy. EPR spectra of the fully reduced complex were obtained by reduction of aliquots with a 1000-fold excess of NADH and a 2000-fold excess of dithionite in the presence of redox mediators as described (*7*). EPR spectra of the enzymes during their reoxidation were obtained by withdrawing samples from the reaction mixture and freezing without further treatment. For the EPR spectra of the connecting fragment of the *E. coli* complex I, an 30 μM aliquot in 50 mM MES/NaOH, pH 6.0, 50 mM NaCl, and 0.1% dodecyl maltoside was reduced with a few grains of dithionite. Samples were frozen in 1:5 isopentane/methylcyclohexane (v/v) at 150 K and stored in liquid nitrogen until analysis. The spectra were recorded with an X-band spectrometer EMX 6/1 (Bruker) equipped with a helium-flow cryostat (Oxford). Spectra were recorded at 9.46 GHz microwave frequency, a modulation amplitude of 0.6 mT, time constant of 0.064 s, and scan rate of 17.9 mT/min. Other parameters are described in the legends to figures. Computer simulations of the spectra were performed as described (*7*), assuming no hyperfine interaction and Gaussian line shape.

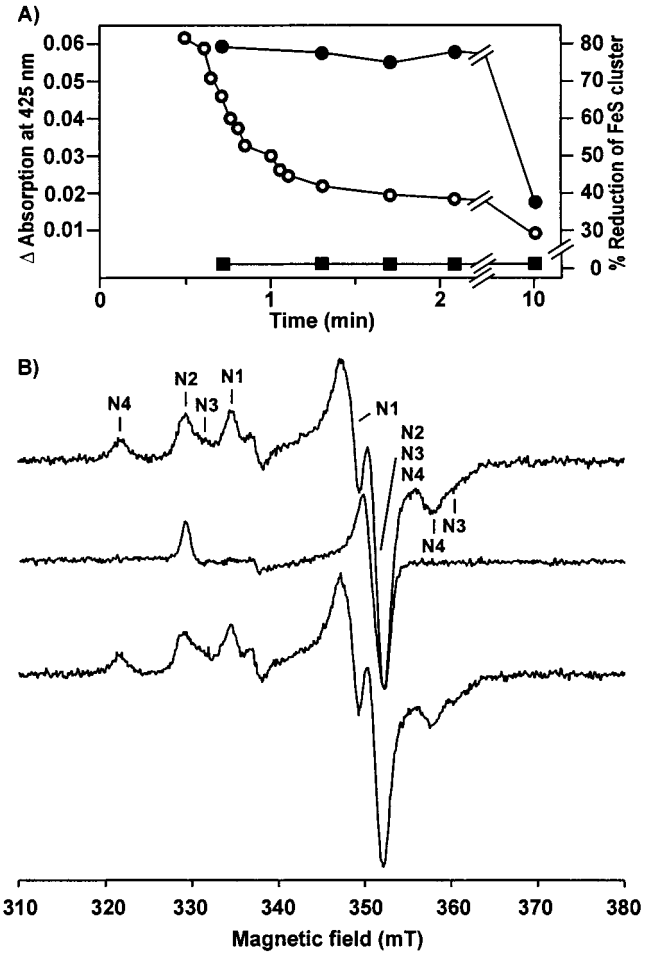

FIGURE 1: Reoxidation of NADH-reduced complex I from *N. crassa* with oxygen. Complex I (7 μM) was reduced with 30 μM NADH at $t = 0$ in a stirred optical cell and exposed to air. (A) Time course of the absorbance at 425 nm (open circles) and degree of reduction of the isopotential FeS clusters (filled squares) and of cluster N2 (filled circles). (B) EPR spectra of an aliquot of the reaction mixture before (upper curve) and after (lower curve) the reaction. Both samples were reduced with an excess of NADH and dithionite as described in Materials and Methods. The middle curve shows an EPR spectrum of the reaction mixture after 40 s of reoxidation. The EPR signals were assigned to the individual FeS clusters according to ref *11*. The corresponding g values are as follows: N1, $g_{x,y,z} = 1.93, 1.93, 2.02$; N2, $g_{x,y,z} = 1.92, 1.92, 2.05$; N3, $g_{x,y,z} = 1.87, 1.93, 2.04$; N4, $g_{x,y,z} = 1.88, 1.92, 2.10$.

Other Analytical Procedures. Non-heme iron and acid-labile sulfide were determined as described (*34*, *35*).

RESULTS

Reaction of NADH-Reduced Complex I with Oxygen. Complex I from *N. crassa* was reduced with a 5-fold excess of NADH, and the reoxidation by oxygen was monitored spectroscopically (Figure 1). Under these conditions the FMN and the isopotential FeS clusters were transiently reduced. Their reoxidation was faster than a few milliseconds and could not be resolved. In contrast, cluster N2 stayed reduced for at least 3 min (Figure 1). Complete reoxidation of this cluster took place within 30 min. A component with negative absorbances at 325 and 425 nm was reoxidized during the first 90 s, while the redox state of the FMN, the isopotential FeS clusters, and cluster N2 did not change (Figures 1 and 2). The chromophore giving rise to these absorbances must therefore belong to a yet unknown redox group. The

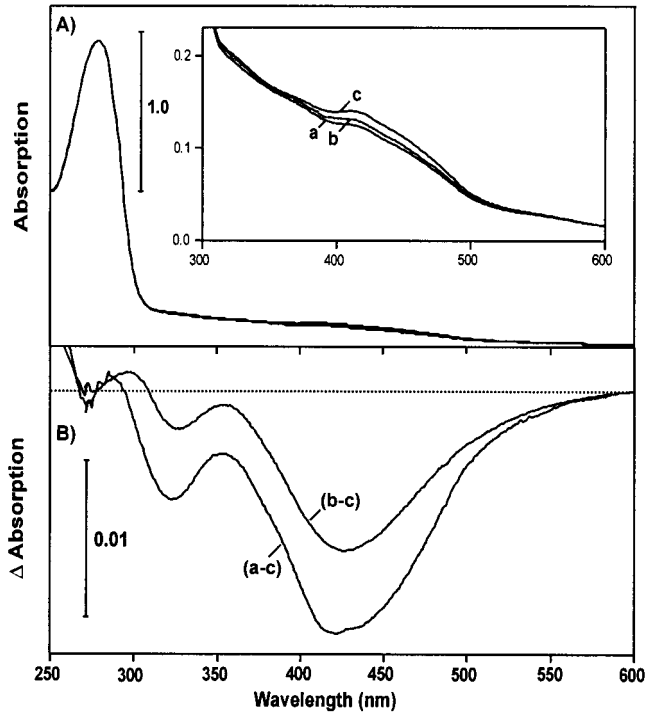

FIGURE 2: UV/vis spectra of 1.7 μM complex I from *N. crassa* at pH 7.5 adjusted to different redox states. (A) Absolute spectra of the complex reduced with 170 μM NADH under anaerobic conditions (a), reduced with 8 μM NADH and 40 s exposure to air (b), and air-oxidized complex I (c). Spectrum b was corrected for the residual absorptions of NAD^+. The inset shows the enlarged region from 300 to 600 nm reflecting the absorbance changes associated with the redox transitions of the cofactors (*15*). (B) Difference spectra of the fully reduced minus air-oxidized complex I (a − c) and of the complex reduced with 8 μM NADH after 40 s exposure to air minus air-oxidized complex I (b − c). The dotted line represents an absorption difference of zero.

difference extinction coefficients of the absorbances at 325 and 425 nm were calculated to be $\Delta\epsilon_{325-600nm} = 3$ mM^{-1} cm^{-1} and $\Delta\epsilon_{425-600nm} = 8$ mM^{-1} cm^{-1}, respectively, considering the residual absorbances after 30 min which stem from a supposedly unknown redox group in the membrane arm of the complex (*15*−*17*).

An aliquot of the reaction mixture was withdrawn prior to and after the reaction, respectively. The samples were reduced with an excess of NADH and dithionite in the presence of redox mediators, and EPR spectra were recorded (Figure 1). After the reaction the amplitude at $g = 1.94$, where the signals of all FeS clusters of complex I overlap, is diminished by approximately 10%. This indicates that the content of the individual FeS clusters has been reduced by roughly 4% in the course of the reaction. However, both spectra can be simulated with the same relative ratio of clusters N1, N2, N3, and N4, namely, 0.7:1:1:1. Therefore, the observed UV/vis absorption does not reflect the decomposition of one of the EPR-detectable FeS clusters. The amplitude of the radical-type signal at $g = 2.00$ (Figure 1B) varied in several repeats of the experiments and did not correlate with the absorption difference at 425 nm.

The peripheral arm of the *N. crassa* complex I which is devoid of cluster N2 (*18*) was reduced with a 4-fold excess of NADH in the same way, and again, the reoxidation by oxygen was monitored spectroscopically. The resulting UV/vis difference spectrum is identical to the one obtained with

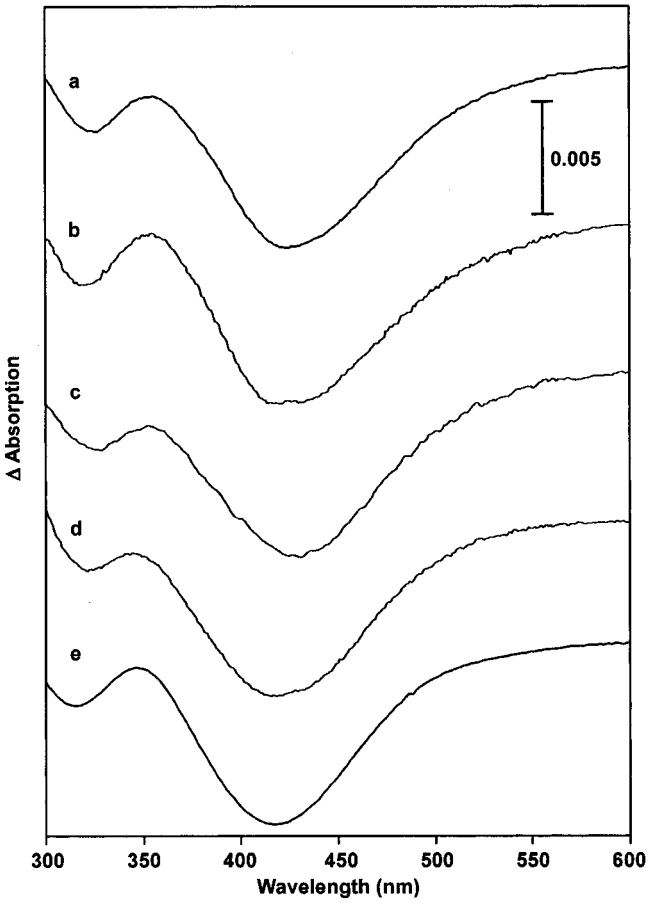

FIGURE 3: UV/vis difference spectra of complex I and related enzymes. Spectra of (a) the novel group in complex I from *N. crassa* (1 μM), (b) the novel group in the peripheral arm of the *N. crassa* complex I (1.4 μM), (c) the dithionite-reduced minus air-oxidized connecting fragment of the *E. coli* complex I (4 μM), (d) the dithionite-reduced minus air-oxidized Ech hydrogenase from *M. barkeri* (0.8 μM), and (e) electrochemically reduced minus electrochemically oxidized 8Fe-ferredoxin from *C. pasteurianum* (0.7 μM). Spectra a and b were obtained as described in the legend to Figure 2. For a better comparison, all enzyme concentrations were calculated to give a difference absorption of 8 mM^{-1} at 425 nm.

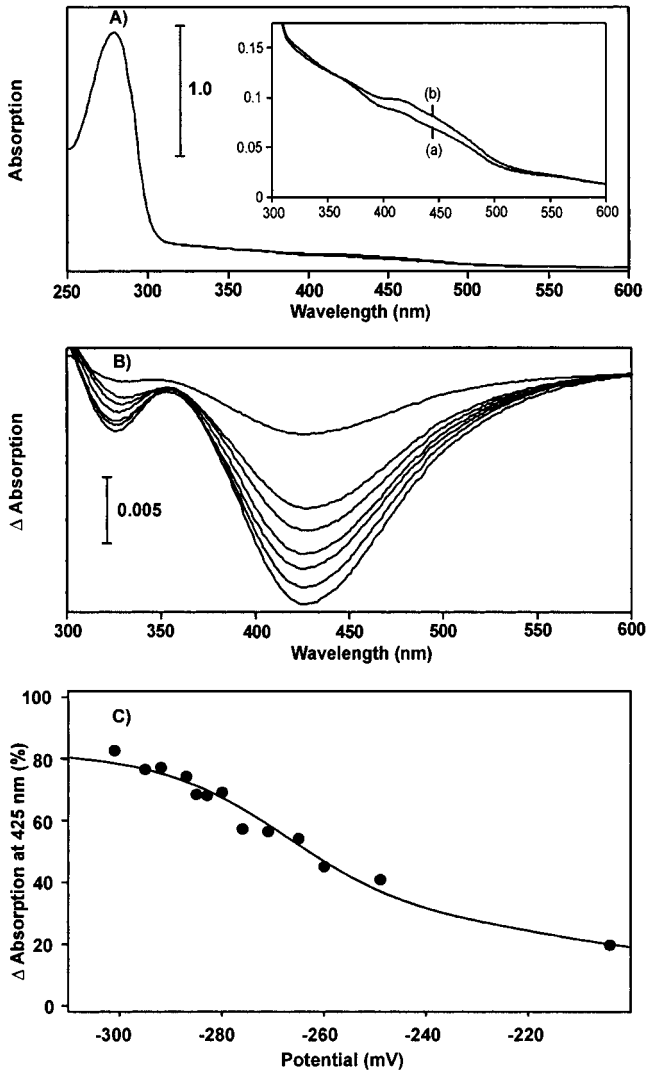

FIGURE 4: Redox titration of the novel group in complex I from *N. crassa*. (A) Absolute spectra of 1.5 μM complex I adjusted to −300 mV (a) and −200 mV (b). The inset shows the enlarged region from 300 to 600 nm. (B) Reduced minus oxidized difference spectra of the complex obtained by the titration. The spectrum obtained at −180 mV is used as the oxidized spectrum. The upper curve (−200 mV minus −180 mV) is dominated by contributions of the unkown redox group in the membrane arm (*15*−*17*). (C) Titration curve corresponding to a best-fit multiple Nernst curve obtained by global analysis for pH 7.8 and by nonlinear regression for pH 7.0, 7.5, and 8.2. The filled circles indicate the absorption at 425 nm at various redox potentials.

complex I (Figure 3). This finding reveals that the novel group is located on one of the peripheral subunits of the complex.

Redox Titration of the Novel Redox Group. To determine the midpoint potential of the novel group, we performed a redox titration in the range from −300 to −200 mV. Global analysis of the spectra obtained at distinct potentials revealed that the negative differences at 325 and 425 nm show the same behavior with respect to the actual redox potential. The titration curve was fitted for one component with a midpoint potential of −270 mV that transfers two electrons (Figure 4). This potential was independent from the applied pH in the range from 7.0 to 8.2. The titration curves did not show any hysteresis upon oxidative and reductive titration, indicating that the reaction was in equilibrium. With the spectra obtained from the peripheral arm of complex I the same pH-independent midpoint potential of the chromophore was determined (data not shown).

Simultaneously, the midpoint potentials of the EPR-detectable FeS clusters were determined by means of EPR spectroscopy to check the setting of the actual potential. The obtained $E_{m,7}$ values (N1, −308 mV; N2, −168 mV; N3, −265 mV; and N4, −268 mV; with $n = 1$ in all cases) are in accordance with the previously determined ones (*11*). The UV/vis difference spectra obtained during the titration under anaerobic conditions (Figure 4) are identical to the difference spectrum obtained by reoxidation of the NADH-reduced enzyme by oxygen from the air (Figure 2). This demonstrates that the observed difference spectrum does not reflect a decomposition of a cofactor or protein caused by its reaction with oxygen.

The Novel Redox Group in the E. coli Complex I. The UV/vis difference spectrum of complex I from *E. coli* at pH 6.0 is dominated by spectral contributions from the FMN at 370 and 455 nm (*36*; Figure 5). Negative absorbances at 330 and 425 nm of the novel group are also present, but they are not as pronounced as in the spectrum of the *N. crassa* complex I at pH 7.5 (Figure 2). This is caused by a larger

Table 1: Homologous Subunits of Complex I from *E. coli* and *N. crassa* and Related Enzymes

N. crassa		*E. coli*			*M. barkeri*	*R. eutropha*	*C. pasteurianum*
complex I	peripheral arm	complex I	NADH dehydrogenase fragment	connecting fragment	Ech hydrogenase	NAD^+-reducing hydrogenase	8Fe-ferredoxin
19 kDa[a]		NuoB[a]		NuoB[a]	EchC[a]	HoxY[a]	
29 kDa	29 kDa	NuoCD (N-term)		NuoCD (N-term)	EchD		
49 kDa	49 kDa	NuoCD (C-term)		NuoCD (C-term)	EchE	HoxH	
24 kDa	24 kDa	NuoE	NuoE			HoxF (N-term)	
51 kDa	51 kDa	NuoF	NuoF			HoxF (C-term)	
78 kDa	78 kDa	NuoG	NuoG			HoxU	
21 kDa[b] plus 33 subunits	21 kDa[b] plus 7 subunits	NuoI[b] plus 7 subunits		NuoI[b]	EchF[b] plus 2 subunits		6 kDa[b]

[a] Subunits homologous to the bovine PSST. [b] Subunits homologous to the bovine TYKY.

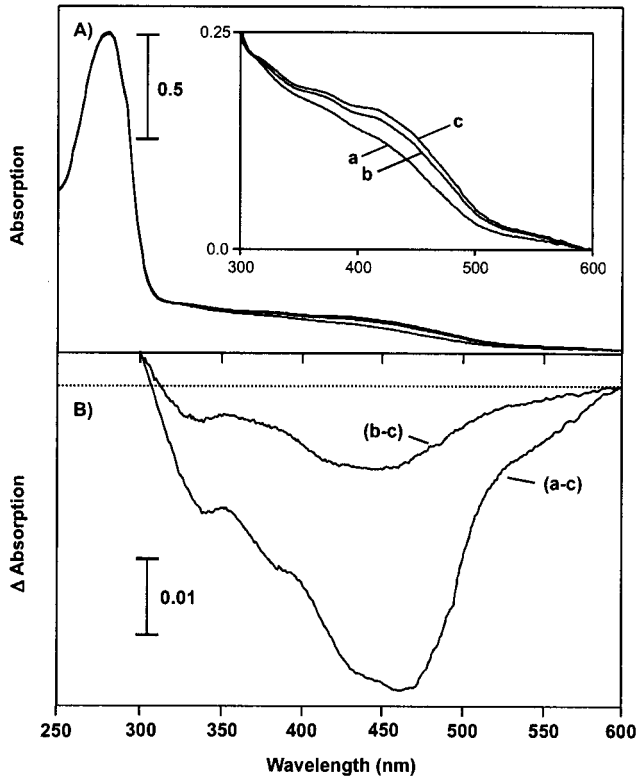

FIGURE 5: UV/vis spectra of 2 μM complex I from *E. coli* at pH 6.0 adjusted to different redox states. (A) Absolute spectra of the complex reduced with 200 μM NADH under anaerobic conditions (a), reduced with 10 μM NADH and 40 s exposure to air (b), and air-oxidized complex I (c). Spectrum b was corrected for the residual absorptions of NAD^+. The inset shows the enlarged region from 300 to 600 nm. (B) Difference spectra of the fully reduced minus air-oxidized complex I (a − c) and of the complex reduced with 10 μM NADH after 40 s exposure to air minus air-oxidized complex I (b − c). The dotted line represents an absorption difference of zero.

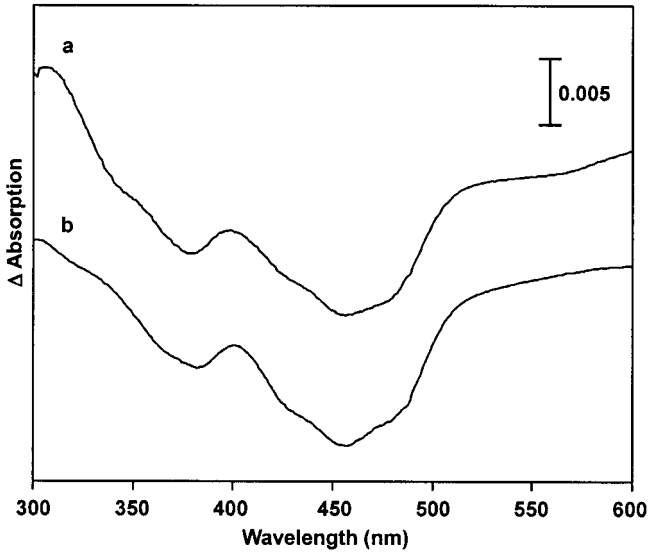

FIGURE 6: UV/vis difference spectra of the NADH dehydrogenase fragment from the *E. coli* complex I (a) and the NAD^+-reducing hydrogenase from *R. eutropha* (b). The NADH-reduced minus air-oxidized difference spectra are shown. The relative intensities of all chromophores did not change during the time course of the reoxidation.

portion of reduced FMN at the lower pH. We were not able to separate the spectra of the novel group and of the FMN kinetically as it was possible with complex I from *N. crassa* (Figure 1). The novel group may be shielded in the eucaryotic complex I by additional subunits causing a lower accessibility to oxygen (*9*). Because of spectral overlap with the FMN, we could not quantify the absorptions at 330 and 425 nm.

We searched for the absorbances of the novel group in fragments of the *E. coli* complex I (Table 1). The connecting fragment lacks the NADH binding site (*7*) and hence was reduced with dithionite. The first spectrum obtained after the excess of dithionite was completely oxidized served as reduced spectrum. The UV/vis difference spectrum showed negative absorptions at 330 and 425 nm with the same relative intensities as obtained with the *N. crassa* complex I (Figure 3). This experiment excludes the possibilty that the UV/vis difference spectrum derives from degraded FMN, because the connecting fragment does not contain FMN (*7*). In contrast, the UV/vis difference spectrum of the NADH dehydrogenase fragment is dominated by the absorbances caused by the FMN at 370 and 455 nm (*36*) and minor absorptions of the binuclear FeS clusters at 420, 470, and 560 nm and of the tetranuclear FeS clusters at 420 nm (*37*−*39*; Figure 6). It did not contain any spectral contributions from the novel group. From these data we conclude that the novel redox group is located in the connecting fragment of the *E. coli* complex I.

UV/Vis Spectra of Related Enzymes. Recently, we have shown that complex I and the [NiFe] hydrogenases share a common ancestor (*40*). The multisubunit membrane-bound Ech hydrogenase from *M. barkeri* is composed of six different subunits, four of them being homologous to subunits of the connecting fragment while two are homologous to hydrophobic subunits of the membrane fragment (Table 1).

The UV/vis reduced minus oxidized difference spectrum of the Ech hydrogenase is comparable to the difference spectrum of the novel group in complex I (Figure 3). Thus, we conclude that the novel redox group of complex I is also present in the Ech hydrogenase.

The NAD^+-reducing hydrogenase from *R. eutropha* contains subunits homologous to the NADH dehydrogenase fragment and to all subunits of the connecting fragment with the exception of the TYKY homologue (Table 1). The UV/vis reduced minus oxidized difference spectrum is devoid of the absorbances of the novel redox group (Figure 6). It resembles the difference spectrum obtained from the NADH dehydrogenase fragment (Figure 6), which emphasizes that these two enzymes represent a conserved protein module (*4*, *40*, *41*). These data indicate that the novel redox group in complex I is most likely located on the homologues of TYKY.

TYKY is a member of a protein family of 8Fe-ferredoxins containing two tetranuclear FeS clusters as the only redox groups (Table 1; *42*). We compared the UV/vis reduced minus oxidized difference spectrum of the *C. pasteurianum* 8Fe-ferredoxin (*26*, *27*) with that of the novel group in complex I. Both spectra proved to be identical (Figure 3). From these data we conclude that the novel group detected in complex I from *N. crassa* and *E. coli* is made up of the two tetranuclear FeS clusters located on subunit Nuo21.3 or NuoI, respectively.

EPR Spectra of the Connecting Fragment. In the reduced state the two FeS clusters in 8Fe-ferredoxins might have a spin $S = {}^1/_2$ or $S = {}^3/_2$ (*43*, *44*). In partially reduced 8Fe-ferredoxins only one of the two FeS clusters is reduced, leading to simple EPR spectra. In this case, both FeS clusters show similar or identical EPR spectra (*45*, *46*). Fully reduced samples, however, exhibit complex spectra with multiple and broad signals of low intensity due to spin coupling of the two reduced clusters (*45*, *46*). The signals of the spin-coupled FeS clusters have been detected in 8Fe-ferredoxins of a few hundred micromolar to some millimolar concentration (*43*−*46*). Due to their low intensity, it is very unlikely to detect these signals in the 7 μM complex I aliquots used for UV/vis spectroscopy (Figure 1). Furthermore, if the clusters would be present, they are most likely covered by the noninteracting FeS clusters.

A preparation of the connecting fragment of the *E. coli* complex I containing the FeS cluster N2 as the known redox group (*7*) was concentrated to 30 μM and reduced by dithionite. The EPR spectrum of this sample shows no signal at 40 K, indicating that the preparation does not contain any binuclear FeS cluster as reported (data not shown). At 13 K the signal of N2 expected to be located in this fragment is detected at $g_{\parallel,\perp} = 2.04, 1.92$ (Figure 7), which is fairly close to the signal of cluster N2 in complex I ($g_{\parallel,\perp} = 2.05, 1.91$). However, some additional, novel signals at $g = 2.086$ and 1.88 are also present in this spectrum.

These signals are only detectable at 13 K and therefore seem to stem from tetranuclear FeS cluster(s). The high-field region of this signal is overlapped by the $g_\perp$ of N2. The signal may have a rhombic symmetry with the g_y absorption completely covered by the $g = 1.92$ signal of cluster N2, or it may have a broad nearly axial symmetry. Our attempts to resolve these signals by a potentiometric titration or by their temperature dependence were so far unsuccessful. These signals have so far not been detected in complex I or a fragment of it. They may arise from the FeS clusters located on the homologue of TYKY. In this case, they might stem from one or both of the FeS clusters of this subunit. In the latter case, the environment of the two clusters might have changed due to the fragmentation of the complex abolishing the coupling between the two clusters. Spin quantitation of the $g_\parallel$ signal of N2 revealed that 80% of this cluster has been lost during isolation. Therefore, we cannot exclude the possibility that the novel EPR signals stem from degraded N2.

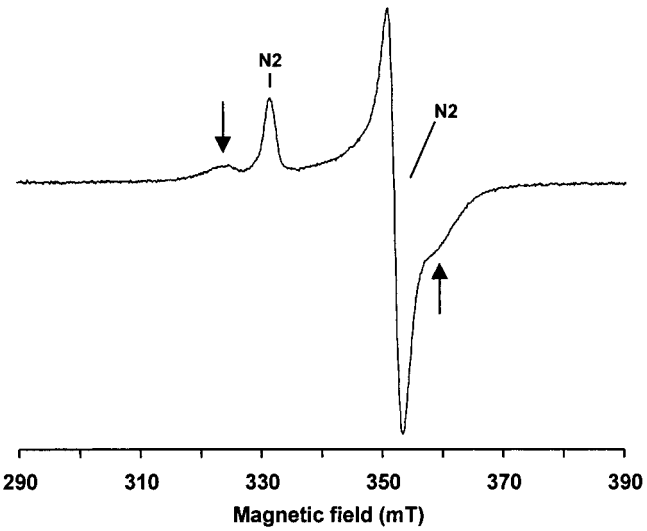

FIGURE 7: EPR spectrum of the connecting fragment of the *E. coli* complex I. A 30 μM aliquot of the connecting fragment was reduced with an excess of dithionite. The spectrum was recorded at 13 K and 5 mW microwave power. Other EPR conditions were as follows: microwave frequency, 9.45 GHz; modulation amplitude, 0.6 mT; time constant, 0.064 s; scan rate, 17.9 mT/min. The spectral positions of the novel absorptions are marked with arrows.

The acid-labile sulfide and non-heme iron contents of five independent preparations of the connecting fragment varied over 5.8−6.0 mol of S^{2-}/mol of protein and 7.6−8.8 mol of iron/mol of protein. The discrepancy between the iron and acid-labile sulfide contents may be explained by unspecifically bound iron or an underestimation of the S^{2-} concentrations. However, both values are inconsistent with the presence of just one tetranuclear FeS cluster in this fragment, especially considering the very low content of cluster N2 in this preparation.

DISCUSSION

The route of electrons through complex I is only partly understood because the exact number of redox groups and their chemical structures are not known. While the function of FMN and the isopotential FeS clusters for the oxidation of NADH has become clear, the transfer of electrons to the membrane arm and further to the substrate ubiquinone is not clear. Especially, the number and type of FeS clusters in subunits homologous to the bovine PSST and TYKY (Table 1), which provide binding motifs for one or two tetranuclear FeS clusters, respectively, are under debate. While one of these subunits binds cluster N2, it has not been clear whether the other subunit contains any FeS cluster at all (*7*, *47*).

Here, we demonstrate that the subunits homologous to TYKY of complex I from *N. crassa* and *E. coli* contain a so

far undetected redox group that corresponds to two tetranuclear FeS clusters. The clusters have been detected in *N. crassa* by two negative peaks at 325 and 425 nm in the UV/vis redox difference spectrum with calculated extinction coefficients of approximately 3 and 8 mM^{-1} cm^{-1}, respectively. It is known that tetranuclear FeS clusters have uncharacteristic optical properties. The very broad absorption peak around 410 nm bleaches approximately 1−2 mM^{-1} cm^{-1} during reduction (*48*, *49*). However, two tetranuclear FeS clusters electronically coupled and arranged as in 8Fe-ferredoxins show characteristic absorption changes with two minima in the difference spectrum (*27*, *50*, *51*).

We attribute these absorbances to the FeS clusters on TYKY because (i) they are present in fragments of complex I from *N. crassa* and *E. coli* that contain this subunit and are missing in a fragment devoid of this subunit, (ii) they are also present in the related Ech hydrogenase containing a homologue of this subunit and are missing in the related NAD^+-reducing hydrogenase devoid of a homologue, and (iii) they are present in an 8Fe-ferredoxin homologous to TYKY containing only two tetranuclear FeS clusters as redox groups. We suggest to refer to these clusters as N6a and N6b.

The UV/vis absorbances of N6a and N6b dominate the spectrum of the *N. crassa* (Figure 2) as well as that of the bovine complex I (Figure 7 in ref *52*). We have taken advantage of this feature to determine the midpoint potential of the FeS clusters as has been reported for 8Fe-ferredoxins (*27*). The UV/vis absorptions of the noninteracting isopotential FeS clusters are too small to interfere with this titration. It was not possible to evaluate a titration of the FeS clusters N1b, N1c, N3, and N4 of the *E. coli* NADH dehydrogenase fragment by means of their UV/vis absorbances due to their small difference extinction coefficients (data not shown). We determined the midpoint potential of N6a and N6b both to be −270 mV, which is in the range of the isopotential FeS clusters. A possible difference in the potential of N6a and N6b smaller than ±20 mV would not be captured by the methods applied. Since the titration curve can be fitted with one component transferring two electrons, it can be assumed that both clusters participate in the redox reaction of complex I. As the midpoint potentials of N6a and N6b are pH-independent, their redox reaction is most likely not directly coupled to proton translocation. The data obtained fit well with the data reported for the two FeS clusters of the *C. pasteurianum* ferredoxin. These clusters have pH-independent and identical midpoint potentials as well (*46*). The redox potential of tetranuclear FeS clusters in soluble ferredoxins may vary from −700 to − 250 mV (*27*, *42*−*46*). The midpoint potential of N6a and N6b is quite positive for FeS clusters of that type. This might be due to the interaction with other subunits within complex I leading to a special conformation of TYKY.

The homologue of TYKY in *Paracoccus denitrificans*, NQO9, was overexpressed and reconstituted with FeS clusters (*47*). It was demonstrated that this subunit indeed can bind two tetranuclear FeS clusters. The EPR signals of these clusters were detected only in the overexpressed and truncated protein but not in the entire complex I in the cytoplasmic membrane (*47*). The FeS clusters give rise to broad signals of nearly axial symmetry at $g = 2.08$, 2.05, and around 1.93 and 1.90. It is discussed that they derive either from two different FeS species or from the presence of spin-coupled clusters as well as noninteracting clusters (*47*). We were able to detect broad EPR signals at 13 K in a fragment of the *E. coli* complex I containing a homologue of TYKY (Figure 7). The different positions of the absorptions could either stem from differences among the species or be due to the artificial systems used to detect the signals.

The EPR spectroscopic characterization of N6a and N6b turns out to be rather difficult, because highly concentrated samples are needed and the absorptions of the noninteracting clusters strongly overlap with the small absorptions of N6a and N6b. So far, we were not able to detect the EPR signals of N6a and N6b in preparations of the entire complex I neither from *N. crassa* nor from *E. coli*. This might be due to a stronger coupling of the clusters in the complex than in the fragment or to the presence of a higher spin ground state. To circumvent these difficulties, the prominent UV/vis difference absorptions of N6a and N6b were most useful for their characterization.

Using complex I from *N. crassa*, we could kinetically separate the UV/vis absorptions of N6a and N6b from the absorptions of all other redox groups by observing their reoxidation. N6a and N6b are reoxidized within 90 s after addition of NADH, while the isopotential FeS clusters reoxidize faster than we were able to resolve with our methods (Figure 1). This means that the electron transfer from N6a and N6b to the isopotential FeS clusters during reoxidation is slower than or equal to the reoxidation rate of N6a and N6b. Because the midpoint potentials of the isopotential FeS clusters and the N6a/N6b couple do not differ, the electron transfer in the reverse direction from the isopotential FeS clusters to N6a and N6b should also be slow. However, the isopotential FeS clusters as well as the N6a/N6b couple are completely reduced by NADH within 5 ms (data not shown). This possibly indicates a branched electron path in complex I behind the FMN with one route leading to the isopotential FeS clusters and the other to clusters N6a and N6b.

Our data imply that cluster N2 must be bound to subunit PSST. The connecting fragment of the *E. coli* complex I contains N2, N6a, and N6b as well as the homologues of PSST and TYKY as sole subunits which contain typical binding motifs for FeS clusters (*7*). Since the homologue of TYKY binds the two novel FeS clusters described above, cluster N2 must be located on the homologue of PSST. This is in accordance with site-directed mutagenesis studies with the complex I from *E. coli* and *Yarrowia lipolytica* (*53*, *54*) and is inconsistent with the proposal that N2 is located on TYKY (*55*). Since PSST contains only three conserved cysteines, the possibility that a neighboring subunit provides the fourth ligand of the FeS cluster cannot be excluded. It has been proposed that TYKY represents a special class of an 8Fe-ferredoxin working as the electrical driving unit for a proton pump (*56*). Sequence comparisons showed that this subunit contains partly conserved amino acids. Therefore, electron transfer involving the FeS clusters on TYKY could be charge compensated by the protonation of the acidic amino acids (*56*). It is an attractive hypothesis, that electron transfer via N6a, N6b, and N2 is required for proton pumping in complex I (*56*, *57*). However, the predicted pH dependence of the midpoint potential of FeS clusters located on TYKY (*56*) was experimentally disproven as shown above.

ACKNOWLEDGMENT

We are grateful to Drs. Bärbel Friedrich, Berlin, and Reiner Hedderich, Marburg, for donating to us their favorite enzymes and to Drs. Jacques Meyer and Jean-Marc Moulis, Grenoble, for sending us UV/vis spectra of the ferredoxin and for helpful discussions. We are also grateful to Dr. Tomoko Ohnishi for helpful discussions and critical reading of the manuscript. We thank Simone Bange for excellent technical assistance.

REFERENCES

1. Weiss, H., Friedrich, T., Hofhaus, G., and Preis, D. (1991) *Eur. J. Biochem. 197*, 563−576.
2. Walker, J. (1992) *Q. Rev. Biophys. 25*, 253−324.
3. Brandt, U. (1997) *Biochim. Biophys. Acta 1318*, 79−91.
4. Friedrich, T., Steinmüller, K., and Weiss, H. (1995) *FEBS Lett. 367*, 107−111.
5. Schulte, U., and Weiss, H. (1995) *Methods Enzymol. 260*, 3−14.
6. Finel, M., Skehel, S. P., Albracht, S. P. J., Fearnley, I. M., and Walker, J. E. (1992) *Biochemistry 31*, 11425−11434.
7. Leif, H., Sled', V. D., Ohnishi, T., Weiss, H., and Friedrich, T. (1995*) Eur. J. Biochem. 230*, 538−548.
8. Guénebaut, V., Vincentelli, R., Mills, D., Weiss, H., and Leonard, K. (1997) *J. Mol. Biol. 275*, 409−418.
9. Guénebaut, V., Schlitt, A., Weiss, H., Leonard, K., and Friedrich, T. (1998) *J. Mol. Biol. 276*, 105−112.
10. Griegorieff, N. (1998) *J. Mol. Biol. 277*, 1033−1046.
11. Wang, D.-C., Meinhardt, S. W., Sackmann, U., Weiss, H., and Ohnishi, T. (1991) *Eur. J. Biochem. 197*, 257−264.
12. Sled', V. D., Friedrich, T., Leif, H., Weiss, H., Meinhardt, S. W., Fukumori, Y., Calhoun, M. W. Gennis, R. B., and Ohnishi, T. (1993) *J. Bioenerg. Biomembr. 25*, 347−357.
13. Sled', V. D., Rudnitzky, N. I., Hatefi, Y., and Ohnishi, T. (1994) *Biochemistry 33*, 10069−10075.
14. Ingledew, W. J., and Ohnishi, T. (1980) *Biochem. J. 186*, 111−117.
15. Schulte, U., Abelmann, A., Amling, N., Brors, B., Friedrich, T., Kintscher, L., Rasmussen, T., and Weiss, H. (1998) *BioFactors 8*, 177−186.
16. Schulte, U., Haupt, V., Abelmann, A., Fecke, W., Brors, B., Rasmussen, T., Friedrich, T., and Weiss, H. (1999) *J. Mol. Biol. 292*, 569−580.
17. Friedrich, T., Brors, B., Hellwig, P., Kintscher, L., Rasmussen, T., Scheide, D., Schulte, U., Mäntele, W., and Weiss, H. (2000) *Biochim. Biophys. Acta 1459*, 305−309.
18. Nehls, U., Friedrich, T., Schmiede, A., Ohnishi, T., and Weiss, H. (1992) *J. Mol. Biol. 227*, 1032−1042.
19. Sackmann, U., Zensen, R., Röhlen, D., Jahnke, U., and Weiss, H. (1991) *Eur. J. Biochem. 200*, 463−469.
20. Braun, M., Bungert, S., and Friedrich, T. (1998) *Biochemistry 37*, 1861−1867.
21. Spehr, V., Schlitt, A., Scheide, D., Guénebaut, V., and Friedrich, T. (1999) *Biochemistry 38*, 16261−16267.
22. Tran-Betcke, A., Warnecke, U., Böcker, C., Zaborosch, C., and Friedrich, B. (1990) *J. Bacteriol. 172*, 2920−2929.
23. Massanz, C., Schmidt, S., and Friedrich, B. (1998) *J. Bacteriol. 180*, 1023−1029.
24. Künkel, A., Vorholt, J. A., Thauer, R. K., and Hedderich, R. (1998) *Eur. J. Biochem. 252*, 467−476.
25. Meuer, J., Bartoschek, S., Koch, J., Künkel, A., and Hedderich, R. (1999) *Eur. J. Biochem. 265*, 325−335.
26. Meyer, J., and Moulis, J.-M. (1981) *Biochem. Biophys. Res. Commun. 103*, 667−673.
27. Moulis, J.-M., and Meyer, J. (1982) *Biochemistry 21*, 4762−4771.
28. Mayhew, S. G., and Massey, V. (1973) *Biochim. Biophys. Acta 315*, 181−190.
29. Burton (1957) *Ergeb. Physiol. 49*, 275.
30. Beechem, J. (1991) *Methods Enzymol. 210*, 37−54.
31. Williams, T., and Kelly, C. (1998) GNUPLOT, Version 3.7.
32. Hendler, R. W., Harmon, P. A., and Levin, I. W. (1994*) Biophys. J. 67*, 2493−2500.
33. Gampp, H., Maeder, M., Meyer, C. J., and Zuberbuehler, A. D. (1985) *Talanta 32*, 95−101.
34. Fish, W. W. (1998) *Methods Enzymol. 158*, 357−364.
35. Beinert, H. (1983) *Anal. Biochem. 131*, 373−376.
36. Gishla, S. (1980) *Methods Enzymol. 66*, 360−373.
37. Malkin, R. (1973) *Iron−Sulfur Proteins* (Lovenberg, W., Ed.) Vol. 2, pp 235−244, Academic Press, Orlando, FL.
38. Dailey, H. A., Finnegan, M. G., and Johnson, M. K. (1994) *Biochemistry 33*, 403−407.
39. Ragan, C. I., Galante, Y. M., Hatefi, Y., and Ohnishi, T. (1982) *Biochemistry 21*, 590−594.
40. Friedrich, T., and Scheide, D. (2000) *FEBS Lett. 479*, 1−5.
41. Pilkington, S. J., Skehel, J. M., Gennis, R. B., and Walker, J. E. (1991) *Biochemistry 30*, 2166−2175.
42. Matsubara, H., and Saeki, K. (1992) *Adv. Inorg. Chem. 38*, 223−280.
43. Palmer, G., and Sands, R. H. (1966) *J. Biol. Chem. 241*, 253−254.
44. Orme-Johnson, W. H., and Beinert, H. (1969) *Biochem. Biophys. Res. Commun. 36*, 337−342.
45. Mathews, R., Charlton, S., Sands, R. H., and Palmer, G. (1974) *J. Biol. Chem. 249*, 4326−4328.
46. Prince, R. C., and Adams, M. W. W. (1987) *J. Biol. Chem. 262*, 5125−5128.
47. Yano, T., Magnitsky, S., Sled', V. D., Ohnishi, T., and Yagi, T. (1999) *J. Biol. Chem. 274*, 28598−28605.
48. Palmer, G., Brintzinger, H., and Estabrook, R. W. (1967) *Biochemistry 6*, 1658−1664.
49. Gutman, M., Singer, T. P., and Beinert, H. (1972) *Biochemistry 11*, 556−562.
50. Butler, J., Henderson, R. A., Armstrong, F. A., and Sykes, A. G. (1979) *Biochem. J. 183*, 471−474.
51. Reeves, R. E., Guthrie, J. D., and Lobelle-Rich, P. (1980) *Exp. Parasitol. 49*, 83−88.
52. Majander, A., Finel, M., and Wikström, M. (1994) *J. Biol. Chem. 269*, 21037−21042.
53. Friedrich, T. (1998) *Biochim. Biophys. Acta 1364*, 134−146.
54. Ahlers, P. M., Zwicker, K., Kerscher, S., and Brandt, U. (2000) *J. Biol. Chem. 275*, 23577−23582.
55. Albracht, S. P. J., and de Jong, A. M. P. (1997) *Biochim. Biophys. Acta 1318*, 92−106.
56. Albracht, S. P. J., and Hedderich, R. (2000) *FEBS Lett. 485*, 1−6.
57. Friedrich, T. (2001) *J. Bioenerg. Biomembr.* (in press).

BI0026977